



Impact of small-scale disturbances on geochemical conditions, biogeochemical processes and element fluxes in surface sediments of the eastern Clarion–Clipperton Zone, Pacific Ocean

Jessica B. Volz¹, Laura Haffert², Matthias Haeckel², Andrea Koschinsky³, and Sabine Kasten^{1,4}

¹Alfred Wegener Institute Helmholtz Centre for Polar and Marine Research, 27570 Bremerhaven, Germany

²GEOMAR Helmholtz Centre for Ocean Research Kiel, 24148 Kiel, Germany

³Department of Physics and Earth Sciences, Jacobs University Bremen, 28759 Bremen, Germany

⁴Faculty of Geosciences, University of Bremen, Klagenfurter Strasse, 28359 Bremen, Germany

Correspondence: Jessica B. Volz (jessica.volz@awi.de)

Received: 12 August 2019 – Discussion started: 20 August 2019

Revised: 18 December 2019 – Accepted: 14 January 2020 – Published: 28 February 2020

Abstract. The thriving interest in harvesting deep-sea mineral resources, such as polymetallic nodules, calls for environmental impact studies and, ultimately, for regulations for environmental protection. Industrial-scale deep-sea mining of polymetallic nodules most likely has severe consequences for the natural environment. However, the effects of mining activities on deep-sea ecosystems, sediment geochemistry and element fluxes are still poorly understood. Predicting the environmental impact is challenging due to the scarcity of environmental baseline studies as well as the lack of mining trials with industrial mining equipment in the deep sea. Thus, currently we have to rely on small-scale disturbances simulating deep-sea mining activities as a first-order approximation to study the expected impacts on the abyssal environment.

Here, we investigate surface sediments in disturbance tracks of seven small-scale benthic impact experiments, which have been performed in four European contract areas for the exploration of polymetallic nodules in the Clarion–Clipperton Zone (CCZ) in the NE Pacific. These small-scale disturbance experiments were performed 1 d to 37 years prior to our sampling program in the German, Polish, Belgian and French contract areas using different disturbance devices. We show that the depth distribution of solid-phase Mn in the upper 20 cm of the sediments in the CCZ provides a reliable tool for the determination of the disturbance depth, which has been proposed in a previous study from the SE Pacific (Paul et al., 2018). We found that the upper 5–15 cm of the sed-

iments was removed during various small-scale disturbance experiments in the different exploration contract areas. Transient transport–reaction modeling for the Polish and German contract areas reveals that the removal of the surface sediments is associated with the loss of the reactive labile total organic carbon (TOC) fraction. As a result, oxygen consumption rates decrease significantly after the removal of the surface sediments, and, consequently, oxygen penetrates up to 10-fold deeper into the sediments, inhibiting denitrification and Mn(IV) reduction. Our model results show that the return to steady-state geochemical conditions after the disturbance is controlled by diffusion until the reactive labile TOC fraction in the surface sediments is partly re-established and the biogeochemical processes commence. While the re-establishment of bioturbation is essential, steady-state geochemical conditions are ultimately controlled by the delivery rate of organic matter to the seafloor. Hence, under current depositional conditions, new steady-state geochemical conditions in the sediments of the CCZ are reached only on a millennium scale even for these small-scale disturbances simulating deep-sea mining activities.

1 Introduction

The accelerating global demand for metals and rare-earth elements drives the economic interest in deep-sea mining (e.g., Glasby, 2000; Hoagland et al., 2010; Wedding et al., 2015).

Seafloor minerals of interest include (1) polymetallic nodules (e.g., Mero, 1965), (2) massive sulfide deposits (e.g., Scott, 1987) and (3) cobalt-rich crusts (e.g., Halkyard, 1985). As the seafloor within the Clarion–Clipperton Zone (CCZ) in the NE Pacific holds one of the most extensive deposits of polymetallic nodules with considerable base metal quantities, commercial exploitation of seafloor mineral deposits may focus on the CCZ (e.g., Mero, 1965; Halbach et al., 1988; Rühlemann et al., 2011; Hein et al., 2013; Kuhn et al., 2017a). The exploration and, ultimately, industrial exploitation of polymetallic nodules demand international regulations for the protection of the environment (e.g., Halfar and Fujita, 2002; Glover and Smith, 2003; Davies et al., 2007; van Dover, 2011; Ramirez-Llodra et al., 2011; Boetius and Haeckel, 2018). The International Seabed Authority (ISA) is responsible for regulating the exploration and exploitation of marine mineral resources as well as for protecting and conserving the marine environment beyond the exclusive economic zones of littoral states from harmful effects (ISA, 2010). The ISA has granted temporal contracts for the exploration of polymetallic nodules in the CCZ, engaging all contract holders to explore resources, test mining equipment and assess the environmental impacts of deep-sea mining activities (ISA, 2010; Lodge et al., 2014; Madureira et al., 2016).

Although a considerable number of environmental impact studies have been conducted in different nodule fields, the prediction of environmental consequences of potential future deep-sea mining is still difficult (e.g., Ramirez-Llodra et al., 2011; Jones et al., 2017; Gollner et al., 2017; Cuvelier et al., 2018). In case of the CCZ, the evaluation of the environmental impact of deep-sea mining activities is challenging due to the fact that baseline data on the natural spatial heterogeneity and temporal variability in depositional conditions, benthic communities and the biogeochemical processes in the sediments are scarce (e.g., Mewes et al., 2014, 2016; Vanreusel et al., 2016; Mogollón et al., 2016; Juan et al., 2018; Volz et al., 2018, 2020; Menendez et al., 2018; Hauquier et al., 2019). In addition, there is no clear consensus on the most appropriate mining techniques for the commercial exploitation of nodules, and technical challenges due to the inaccessibility of nodules at great water depths between 4000 and 5000 m have limited the deployment of deep-sea mining systems until today (e.g., Chung, 2010; Jones et al., 2017).

The physical removal of nodules as hard-substrate habitats has severe consequences for the nodule-associated sessile fauna as well as the mobile fauna (Bluhm, 2001; Smith et al., 2008; Purser et al., 2016; Vanreusel et al., 2016). With slow nodule growth rates of a few millimeters per million years (e.g., Halbach et al., 1988; Kuhn et al., 2017a), the deep-sea fauna may not recover for millions of years (Vanreusel et al., 2016; Jones et al., 2017; Gollner et al., 2017; Stratmann et al., 2018). In addition to the removal of deep-sea fauna as well as seafloor habitats, the exploitation of nodules is associated with (1) the removal, mixing and re-suspension of the upper 4 cm to more than several tens of centimeters of the sedi-

ments; (2) the re-deposition of material from the suspended sediment plume; and (3) potentially also the compaction of the surface sediments due to weight of the nodule collector (Thiel and Forschungsverband Tiefsee-Umweltschutz, 2001; Oebius et al., 2001; König et al., 2001; Grupe et al., 2001; Radziejewska, 2002; Khripounoff et al., 2006; Cronan et al., 2010; Paul et al., 2018; Gillard et al., 2019). The wide range of estimates for the disturbance depth may be associated with (1) various devices used for the deep-sea disturbance experiments (Brockett and Richards, 1994; Oebius et al., 2001; Jones et al., 2017), (2) distinct sediment properties in different nodule fields of the Pacific Ocean (e.g., Cronan et al., 2010; Hauquier et al., 2019) and (3) different approaches for the determination of the disturbance depth (e.g., Oebius et al., 2001; Grupe et al., 2001; Khripounoff et al., 2006). Based on the observation that bulk solid-phase Mn contents decrease over depth in the surface sediments of the Disturbance and Recolonization Experiment (DISCOL) area in the Peru Basin, SE Pacific, Paul et al. (2018) have suggested that the depth distribution of solid-phase Mn and associated metals (e.g., Mo, Ni, Co, Cu) could be used to trace the sediment removal by disturbances. In addition, other solid-phase properties such as total organic carbon (TOC) contents, porosity and radioisotopes may be suitable for the determination of the disturbance depth.

The most reactive TOC compounds, found in the bioturbated uppermost sediment layer, are the main drivers for early diagenetic processes (e.g., Froelich et al., 1979; Berner, 1981) and are expected to be removed during mining activities (König et al., 2001). Thus, strong biogeochemical implications can be expected in the sediments after deep-sea mining activities. König et al. (2001) have applied numerical modeling to study the consequences of the removal of the upper 10 cm of the sediments in the DISCOL area. They showed that the degradation of TOC during aerobic respiration, denitrification and Mn(IV) reduction may be decreased for centuries, increasing the oxygen penetration depth (OPD).

Here, we investigate the impact of various small-scale disturbances on geochemical conditions, biogeochemical processes and element fluxes in surface sediments of the CCZ. These small-scale disturbance tracks were created up to 37 years ago in four different European contract areas for the exploration of polymetallic nodules, including the German BGR (Bundesanstalt für Geowissenschaften und Rohstoffe) area, the Belgian GSR (Global Sea Mineral Resources NV) area, the French IFREMER (Institut Français de Recherche pour l'Exploitation de la Mer) area and the Polish IOM (Interoceanmetal) area. In order to determine the disturbance depths of the different small-scale disturbances in the different European contract areas, we correlate the depth distributions of solid-phase Mn and TOC between disturbed sites and undisturbed reference sites using the Pearson product-moment correlation coefficient. On this basis, we (1) assess the short- and long-term consequences of small-scale distur-

bances on redox zonation and element fluxes and (2) determine how much time is needed for the re-establishment of a new steady-state geochemical system in the sediments after the disturbances. Our work includes pore-water and solid-phase analyses as well as the application of a transient one-dimensional transport-reaction model.

2 Material and methods

As part of the European JPI Oceans pilot action “Ecological aspects of deep-sea mining (MiningImpact)”, multiple-corer (MUC) and gravity-corer (GC) sediment cores were taken during the RV *SONNE* cruise SO239 in March–April 2015 from undisturbed sites in various European contract areas for the exploration of polymetallic nodules (Fig. 1; Table 1; Martínez Arbizu and Haeckel, 2015). These undisturbed reference sites were chosen in close proximity (<5 km) to small-scale disturbance experiments for the simulation of deep-sea mining, which were created up to 37 years ago and revisited during cruise SO239 (Table 1; see Sect. 2.1.1.; Martínez Arbizu and Haeckel, 2015). The sampling of sediments in the disturbance tracks of these experiments was conducted by video-guided push coring (PC) between 1 d and 37 years after the initial disturbances using the ROV *Kiel 6000* (Table 1; Fig. 2; Martínez Arbizu and Haeckel, 2015).

The different investigated European contract areas within the CCZ include the BGR, IOM, GSR and IFREMER areas. Comprehensive pore-water and solid-phase analyses on the MUC and GC sediment cores from undisturbed sites have been conducted in previous baseline studies and are presented elsewhere (Volz et al., 2018, 2020). These analyses include the determination of pore-water oxygen; NO_3^- , Mn^{2+} and NH_4^+ concentrations; and TOC contents for MUC and GC sediment cores (Volz et al., 2018) as well as solid-phase bulk Mn contents for the MUC sediment cores (Volz et al., 2020). In the framework of this study, we used these previously published pore-water and solid-phase data as undisturbed reference data for geochemical conditions and sediment composition (Table 1). On this basis, here we investigate seven small-scale disturbances for the simulation of deep-sea mining (Table 1; see Sect. 2.1.1.; Martínez Arbizu and Haeckel, 2015).

2.1 Site description

The CCZ is defined by two transform faults, the Clarion Fracture Zone in the north and the Clipperton Fracture Zone in the south, and covers an area of about $6 \times 10^6 \text{ km}^2$ (Fig. 1; e.g., Halbach et al., 1988). The sediments at the investigated sites (Table 1) are dominated by clayey siliceous oozes, with Mn nodules varying in size (1–10 cm) and spatial density ($0\text{--}30 \text{ kg m}^{-2}$) at the sediment surface (Berger, 1974; Kuhn et al., 2012; Mewes et al., 2014; Volz et al., 2018). In order to characterize the investigated sediments with respect to redox

zonation, sedimentation rates, fluxes of particulate organic carbon (POC) to the seafloor and bioturbation depths, we summarized these key parameters, which are originally presented elsewhere, in Table 2 (Volz et al., 2018). Steady-state transport-reaction models have shown that aerobic respiration is the dominant biogeochemical process at all investigated sites, consuming more than 90 % of the organic matter delivered to the seafloor (Mogollón et al., 2016; Volz et al., 2018). Below the OPD at more than 0.5 m depth, Mn(IV) and nitrate reduction succeed in the suboxic zone, where oxygen and sulfide are absent (e.g., Mewes et al., 2014; Mogollón et al., 2016; Kuhn et al., 2017b; Volz et al., 2018). At several sites investigated in this study, including the BGR “reference area” (BGR-RA) and IOM sites, decreasing Mn^{2+} concentrations at depth are probably associated with the oxidation of Mn^{2+} by upwardly diffusing oxygen circulating through the underlying basaltic crust (Mewes et al., 2016; Kuhn et al., 2017b; Volz et al., 2018).

2.1.1 Small-scale disturbances

Since the 1970s, several comprehensive environmental impact studies of deep-sea mining simulations have been carried out in the CCZ, including the Benthic impact experiment (BIE; e.g., Trueblood and Ozturgut, 1997; Radziejewska, 2002) and the Japan deep-sea impact experiment (JET; Fukushima, 1995). In addition, numerous small-scale seafloor disturbances have been carried out in the CCZ in the past 40 years using various tools such as epibenthic sledge (EBS) and dredges (e.g., Vanreusel et al., 2016; Jones et al., 2017). The EBS is towed along the seabed for the collection of benthic organisms (and nodules), thereby also removing the upper few centimeters of the sediments (e.g., Brenke, 2005). In 2015, some of these disturbances that were up to 37 years old were revisited as part of the BMBF–EU JPI Oceans pilot action “Ecological aspects of deep-sea mining (MiningImpact)” project in order to evaluate the long-term consequences of such small-scale disturbances on the abyssal benthic ecosystem (Table 1; Fig. 2; Martínez Arbizu and Haeckel, 2015). For comparison, DISCOL, which was conducted in a nodule field in the Peru Basin (PB) in 1989, was revisited as part of MiningImpact (Boetius, 2015; Greinert, 2015). In the framework of DISCOL, a seafloor area of $\sim 11 \text{ km}^2$ was disturbed with a plow harrow. The impact of the DISCOL experiment was studied 0.5, 3 and 7 years after the disturbance had been set (e.g., Thiel and Forschungsverband Tiefsee-Umweltschutz, 2001). Furthermore, new small-scale disturbance tracks were created during SO239 in the BGR-RA and in the GSR area “B6” using an EBS in order to add also initial temporal datasets (Table 1; Fig. 2; Martínez Arbizu and Haeckel, 2015). The EBS weighed about 400 kg and created a disturbance track of about 1.5 m width (Brenke, 2005). The fresh EBS disturbance tracks in the BGR-RA and GSR areas were revisited 1 d after their creation. Eight months prior to the cruise SO239, towed

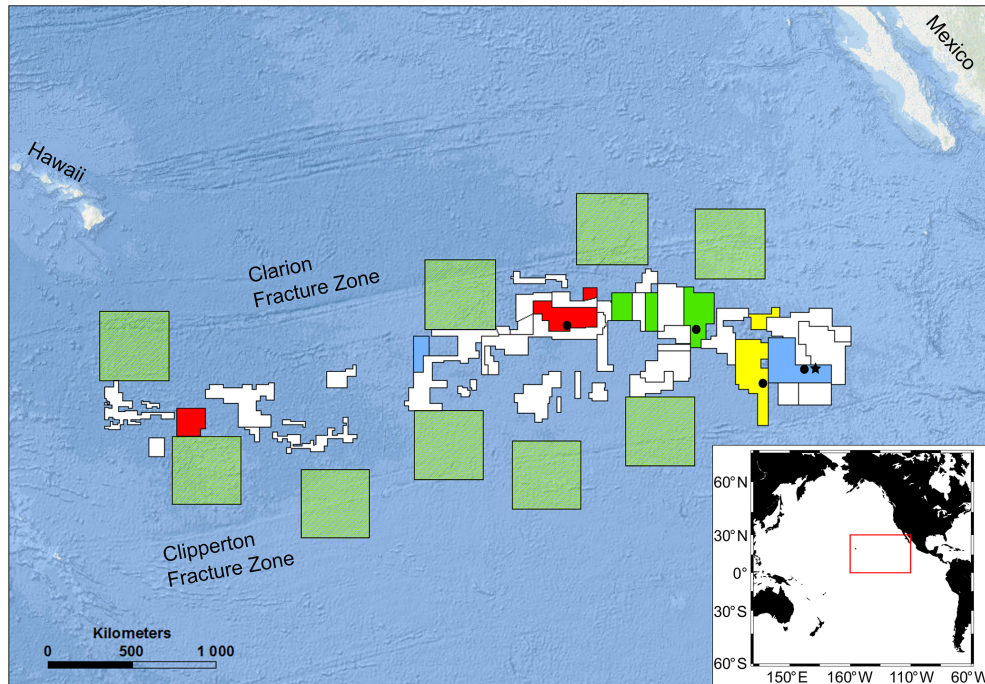


Figure 1. Sampling sites (black circles; black star) in various European contract areas for the exploration of manganese nodules within the Clarion–Clipperton Zone (CCZ). Investigated stations are located in the German BGR area (blue), eastern European IOM area (yellow), Belgian GSR area (green) and French IFREMER area (red). The two stations within the German BGR area are located in the “prospective area” (BGR-PA; black star) and in the “reference area” (BGR-RA; black circle). The contract areas granted and governed by the International Seabed Authority (ISA; white areas) are surrounded by nine areas of particular environmental interest (APEIs), which are excluded from any mining activities (green shaded squares). Geographical data provided by the ISA.

Table 1. MUC and PC cores investigated in this study, including information on geographic position, water depth, type and age of the disturbances (years: yr; months: mth; days: d).

Area	Site SO239-	Coring device	Disturbance device and type	Disturbance age	Latitude (N)	Longitude (W)	Water depth (m)
BGR-PA	39	MUC	–	–	11°50.64′	117°03.44′	4132.0
BGR-PA	41	PC	EBS ¹	3 yr	11°50.92′	117°03.77′	4099.2
BGR-RA	62	GC	–	–	11°49.12′	117°33.22′	4312.2
BGR-RA	64	PC	EBS ²	1 d	11°48.27′	117°30.18′	4332
BGR-RA	66	MUC	–	–	11°49.13′	117°33.13′	4314.8
IOM	84	MUC	–	–	11°04.73′	119°39.48′	4430.8
IOM	87	GC	–	–	11°04.54′	119°39.83′	4436
IOM	101	PC	IOM-BIE ³	20 yr	11°04.38′	119°39.38′	4387.4
GSR	121	MUC	–	–	13°51.25′	123°15.3′	4517.7
GSR	131	PC	EBS ²	1 d	13°52.38′	123°15.1′	4477.6
GSR	141	PC	Dredge ⁴	8 mth	13°51.95′	123°15.33′	4477
IFREMER	157	PC	Dredge ⁵	37 yr	14°02.06′	130°07.23′	4944.5
IFREMER	161	PC	EBS ¹	3 yr	14°02.20′	130°05.87′	4999.1
IFREMER	175	MUC	–	–	14°02.45′	130°05.11′	5005.5

¹ Epibenthic sledge (EBS) during BIONOD cruises in 2012 aboard *L’Atalante* (Brenke, 2005; Rühlemann et al., 2013; Menot et al., 2013). ² Epibenthic sledge (EBS) during RV *SONNE* cruise SO239 in 2015 (Brenke, 2005; Martínez Arbizu and Haeckel, 2015). ³ Benthic impact experiment (BIE); disturbance created with the deep-sea sediment re-suspension system (DSSRS; e.g., Brockett and Richards, 1994; Kotlinski and Stoyanova, 1998). ⁴ Towed dredge sampling during GSR cruise in 2014 aboard MV *Mt. Mitchell* (Jones et al., 2017). ⁵ Towed dredge sampling by the Ocean Minerals Company (OMCO) in 1978 aboard *Hughes Glomar Explorer* (Morgan et al., 1993; Spickermann, 2012).

Table 2. Information of sedimentation rate (Sed. rate), flux of particulate organic carbon (POC) to the seafloor, bioturbation depth (Bioturb. depth), and oxygen penetration depth (OPD) based on GC cores from the investigated sites and determined in the study by Volz et al. (2018). Information for the BGR-PA area is taken from an adjacent site (A5-2-SN; 11°57.22' N, 117°0.42' W) studied by Mewes et al. (2014) and Mogollón et al. (2016).

Area	Sed. rate (cm kyr ⁻¹)	POC flux (mg C _{org} m ⁻² d ⁻¹)	Bioturb. depth (cm)	OPD (m)
BGR-PA	~ 0.53 ^a	~ 6.9 ^a	~ 5 ^a	~ 2 ^{a,b}
BGR-RA	0.65	1.99	7	0.5
IOM	1.15	1.54	13	3
GSR	0.21	1.51	8	> 7.4
IFRE-1	0.64	1.47	7	4.5
IFRE-2	0.48	1.5	8	3.8
APEI3	0.2	1.07	6	> 5.7

^a Mogollón et al. (2016). ^b Mewes et al. (2014).

dredge sampling was performed in the GSR area by the Belgian contractor (Martínez Arbizu and Haeckel, 2015; Jones et al., 2017). During the BIONOD cruises aboard RV *L'Atalante* in 2012, the same EBS setup as used during cruise SO239 was deployed in the BGR “prospective area” (BGR-PA) and in the IFREMER area (Table 1; Rühlemann et al., 2013; Menot et al., 2013; Martínez Arbizu and Haeckel, 2015). In 1995, the deep-sea sediment re-suspension system (DSSRS) was used during the IOM-BIE (Benthic Impact Experiment) disturbance in the IOM area (Table 1; e.g., Kotlinski and Stoyanova, 1998). The DSSRS weighed 3.2 t under normal atmospheric pressure and was designed to dredge the seafloor while producing a re-suspended particle plume about 5 m above the seafloor (Brockett and Richards, 1994; Sharma, 2001). Based on the dimensions of the DSSRS device, the disturbance track created during the IOM-BIE disturbance experiment is about 2.5 m wide (Fig. 2; Brockett and Richards, 1994). In 1978, the Ocean Mineral Company (OMCO) created disturbance tracks in the French IFREMER area by towed dredge sampling (Table 1; e.g., Spickermann, 2012).

2.2 Sediment sampling and solid-phase analyses

ROV-operated push cores were sampled at intervals of 1 cm for solid-phase analyses. Bulk sediment data and TOC contents have been corrected after Kuhn (2013) for the interference of the pore-water salt matrix with the sediment composition (Volz et al., 2018). The mass percentage of the pore water was determined gravimetrically before and after freeze-drying of the wet sediment samples. The salt-corrected sediment composition c' was calculated from the measured solid-phase composition c using the mass percentage of H₂O of the wet sediment (w), which contains 96.5 %

H₂O (Eq. 1):

$$c' = c \cdot \frac{100}{100 - \left(100 \cdot \frac{(w \cdot \frac{100}{96.5}) - w}{100 - w} \right)}. \quad (1)$$

2.2.1 Total acid digestions

Total acid digestions were performed in the microwave system MARS Xpress (CEM) after the protocols by Kretschmer et al. (2010) and Nöthen and Kasten (2011). Approximately 50 mg of freeze-dried, homogenized bulk sediment was digested in an acid mixture of 65 % sub-boiling distilled HNO₃ (3 mL), 30 % sub-boiling distilled HCl (2 mL) and 40 % Suprapur® HF (hydrofluoric acid; 0.5 mL) at ~ 230 °C. Digested solutions were fumed off to dryness; the residue was re-dissolved under pressure in 1 M HNO₃ (5 mL) at ~ 200 °C and then filled up to 50 mL with 1 M HNO₃. Total bulk Mn and Al contents were determined using inductively coupled plasma optical emission spectrometry (ICP-OES; IRIS Intrepid ICP-OES Spectrometer, Thermo Elemental). Based on the standard reference material NIST 2702, accuracy and precision of the analysis were 3.7 % and 3.5 % for Mn, respectively ($n = 67$).

2.2.2 Total organic carbon

Total organic carbon (TOC) contents were determined using an Eltra CS-2000 element analyzer. Approximately 100 mg of freeze-dried, homogenized sediment was transferred into a ceramic cup and decalcified with 0.5 mL of 10 % HCl at 250 °C for 2 h before analysis. Based on an in-house reference material, precision of the analysis was better than 3.7 % ($n = 83$).

2.3 Pearson correlation coefficient

In order to determine the disturbance depths, solid-phase bulk Mn contents were correlated between disturbed sediments and undisturbed reference sediments using the Pearson

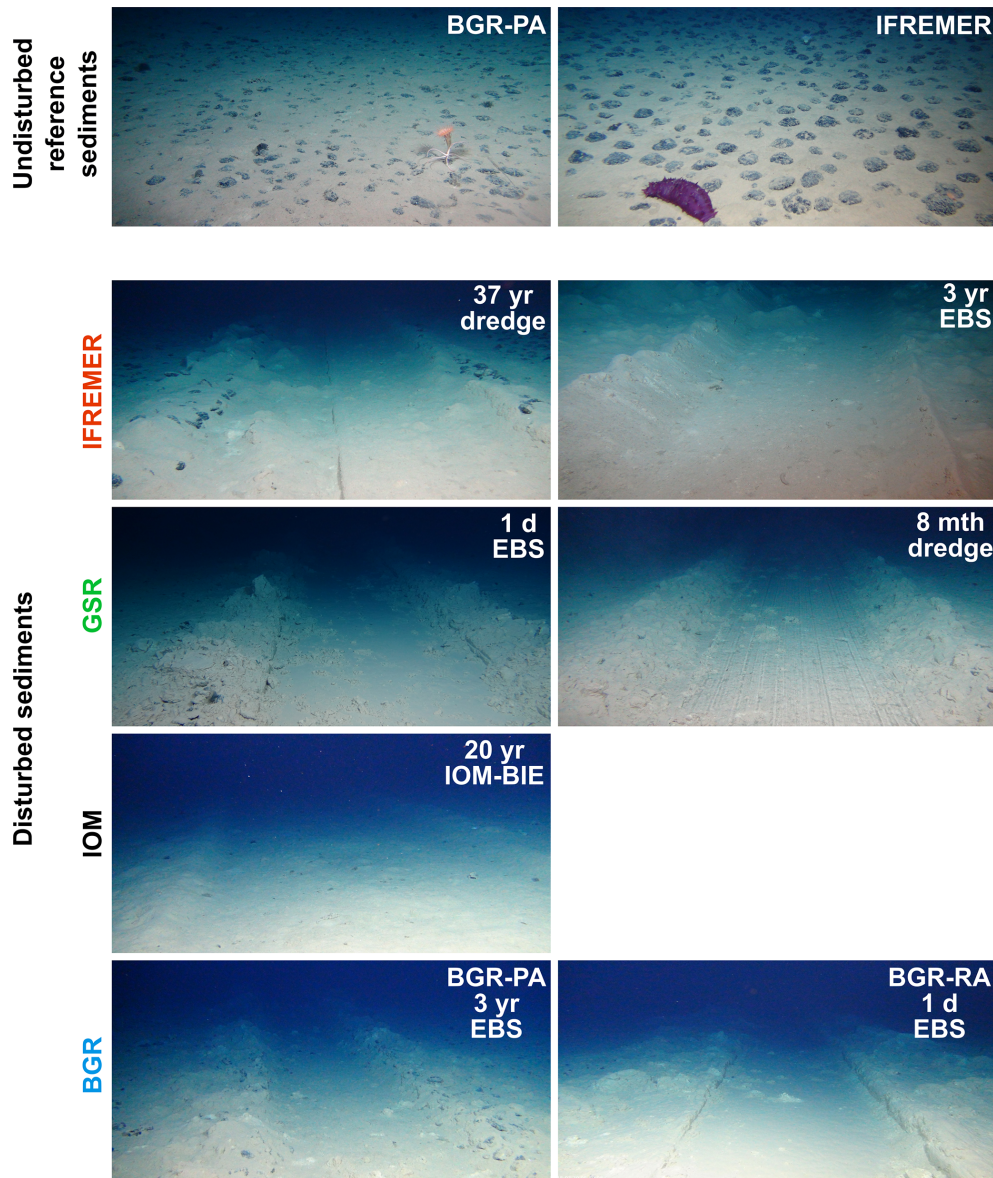


Figure 2. Examples of undisturbed reference sediments in the German BGR-PA area and the French IFREMER area and pictures of small-scale disturbances for the simulation of deep-sea mining within the CCZ, which are investigated in the framework of this study (years: yr; months: mth; days: d). Copyright: ROV *KIEL 6000* Team, GEOMAR Helmholtz Centre for Ocean Research Kiel, Germany.

product–moment correlation coefficient r (Eq. 1; Table 1; Pearson, 1895). The Pearson correlation coefficient is a statistical measure of the linear relationship between two arrays of variables, with

$$r_{xy} = \frac{\sum_{i=1}^n (x_i - \bar{x})(y_i - \bar{y})}{\sqrt{\sum_{i=1}^n (x_i - \bar{x})^2 \sum_{i=1}^n (y_i - \bar{y})^2}}, \quad (2)$$

where n is the sample size, x and y are individual sample points, and \bar{x} and \bar{y} are the sample means $\bar{x} = \frac{1}{n} \sum_{i=1}^n x_i$ and $\bar{y} = \frac{1}{n} \sum_{i=1}^n y_i$.

While the solid-phase bulk Mn contents of the disturbed sediments were determined in the framework of this study,

solid-phase bulk Mn contents from undisturbed reference sediments were taken from Volz et al. (2020). The highest positive linear correlations of solid-phase Mn contents ($r_{Mn} \sim 1$) between the disturbed sites and the respective undisturbed reference sites (Table 1) were used to determine the depths of the disturbances. In a second step, the same correlation was applied to the TOC contents (r_{TOC}) in order to verify the depth of disturbance. While the TOC contents in the disturbed sediments were determined in the framework of this study, TOC contents from undisturbed reference sediments were taken from Volz et al. (2018).

2.4 Geochemical model setup and reaction network

A transient one-dimensional transport-reaction model (Eq. 3; e.g., Boudreau, 1997; Haeckel et al., 2001) was used (1) to assess the impact of small-scale disturbances on biogeochemical processes, geochemical conditions and element fluxes in sediments of the CCZ and (2) to estimate the time required to establish a new steady-state geochemical system after a small-scale disturbance. We applied a transient transport-reaction model for the sites in the BGR-RA and IOM areas (Table 1). These sites were chosen due to distinctively different sedimentation rates and OPD (Table 2). We adapted the code of the steady-state transport-reaction model, which was originally presented by Volz et al. (2018), and used pore-water oxygen, NO_3^- , Mn^{2+} and NH_4^+ data as well as TOC contents of GC sediment cores from the same study as undisturbed reference data (Tables 1, 2). Thus, the model parameters and baseline input data used for the transient transport-reaction model are the same as presented in the study by Volz et al. (2018). The transient transport-reaction model consists of four aqueous species (O_2 , NO_3^- , Mn^{2+} , NH_4^+), four solid species (TOC_1 , TOC_2 , TOC_3 , MnO_2) and six reactions (R1–R6; Supplement Table S1), with

$$\frac{\partial(\theta_i C_{i,j})}{\partial t} = \frac{\partial D_{i,j} \theta_i (\partial C_{i,j} / \partial z)}{\partial z} - \frac{\partial \omega_i \theta_i C_{i,j}}{\partial z} + \alpha_i \theta_i (C_{i,j} - C_{0,j}) + \theta_i \sum R_{i,j}, \quad (3)$$

where z is sediment depth, and subscripts i and j represent depth and species dependence, respectively; aqueous or solid species concentration is denoted by C (Table S2), and D is, in the case of solutes, the effective diffusive mixing coefficient, which has been corrected for tortuosity ($D_{m,i,j}$; Boudreau, 1997). In the case of solids, D represents the bioturbation coefficient (B_i ; Eq. 4), ϑ is the volume fraction representing the porosity φ for the aqueous phase and $1 - \varphi$ for the solid phase, the velocity of either the aqueous (v) or the solid phase (w) is denoted by the symbol ω , α_i is the bioirrigation coefficient (0 for solid species; Eq. 5), and $\sum R_{i,j}$ is the sum of the reactions affecting the given species.

The bioturbation and bioirrigation profiles, i.e., biologically induced mixing of sediment and pore water, respectively, are represented by a modified logistic function:

$$B_i = B_0 \exp\left(\frac{z_{\text{mix}} - z_i}{z_{\text{att}}}\right) / \left(1 + \exp\left(\frac{z_{\text{mix}} - z_i}{z_{\text{att}}}\right)\right), \quad (4)$$

$$\alpha_i = \alpha_0 \exp\left(\frac{z_{\text{mix}} - z_i}{z_{\text{att}}}\right) / \left(1 + \exp\left(\frac{z_{\text{mix}} - z_i}{z_{\text{att}}}\right)\right), \quad (5)$$

where α_0 and B_0 are constants indicating the maximum bioirrigation and bioturbation intensity at the sediment–water interface (SWI), the depth where the bioturbation and bioirrigation intensity is halved is denoted by z_{mix} , and the attenuation of the biogenically induced mixing with depth is controlled by z_{att} .

Assuming steady-state compaction, the model applies an exponential function that is parameterized according to the available porosity data at each station (e.g., Berner, 1980; Supplement Fig. S1):

$$\varphi_i = \varphi_\infty (\varphi_0 - \varphi_\infty) \exp(-\beta z), \quad (6)$$

where φ_∞ is the porosity at the “infinite depth”, at which point compaction is completed, φ_0 is the porosity at the sediment water interface ($z = 0$), and β is the porosity-attenuation coefficient.

Organic matter was treated in three reactive fractions (3G-model) with first-order kinetics. The rate expressions for the reactions (R1–R6) include inhibition terms, which are listed together with the rate constants (Table S3).

Based on the Pearson correlation coefficient r_{Mn} , we removed the upper 7 cm of sediments in the transport-reaction model for the IOM-BIE site and the upper 10 cm of sediments in the transport-reaction model for the BGR-RA site. Due to the lack of data on the re-establishment of bioturbation, i.e., the recovery of the bioturbation “pump” after small-scale disturbance experiments, we tested the effect of different bioturbation scenarios in the transport-reaction model. For the different post-disturbance bioturbation scenarios, we assumed that bioturbation is inhibited immediately after the disturbance with a linear increase to undisturbed reference bioturbation coefficients (Volz et al., 2018). Based on the work by Miljutin et al. (2011) and Vanreusel et al. (2016), we assumed that bioturbation should be fully re-established after 100, 200 and 500 years. As the modeling results for the different time spans were almost identical, we only present here the model that assumes that bioturbation is at pre-disturbance intensity 100 years after the impact (Volz et al., 2018; Table S2). We applied the transient transport-reaction model under the assumption that the sedimentation rates as well as the POC fluxes to the seafloor remain constant over time (Table 2). The model was coded in MATLAB, with a discretization and reaction setup closely following the steady-state model (Volz et al., 2018).

3 Results

3.1 Characterization of disturbed sites

Most of the small-scale disturbances investigated in the framework of this study were created with an EBS (Table 1; Fig. 2). Based on the visual impact inspection of the EBS disturbance tracks in the CCZ, the sediments were mostly pushed aside by the EBS and piled up next to the left and right side of the tracks (Fig. 2). In particular, the freshly created 1 d old EBS tracks in the BGR-RA and GSR areas indicate that the sediments were mostly scraped off and accumulated next to the freshly exposed sediment surfaces (Fig. 2). Small sediment lumps occur on top of the exposed sediment surfaces on the EBS tracks, which indicates that some sedi-

Table 3. Calculated Pearson correlation coefficients r_{Mn} and r_{TOC} for the determination of the disturbance depth of various small-scale disturbances investigated in the framework of this study (compare Table 1). For both correlations, the highest positive linear Pearson coefficient for solid-phase Mn contents ($r_{\text{Mn}} \sim 1$) between the disturbed sites and the respective undisturbed reference sites was used.

Exploration area	Disturbance device and type	Disturbed site SO239-	Reference site SO239-	r_{Mn}	Disturbance depth (cm)	r_{TOC}
BGR-PA	EBS	41	39	0.86	5	–
BGR-RA	EBS	64	66	0.82	15	–0.4
IOM	IOM-BIE	101	87	0.97	7	0.77
GSR	EBS	131	121	0.72	6	0.88
GSR	Dredge	141	121	0.88	6	0.91
IFREMER	Dredge	157	175	0.74	10	0.73
IFREMER	EBS	161	175	0.93	7	0.74

ment slid off from the adjacent flanks of the sediment accumulation after the disturbances (Fig. 2). However, the mostly smooth sediment surfaces of the EBS tracks suggest that sediment mixing during the EBS disturbance experiments may be mostly negligible (Fig. 2; Table 1). In the 8-month-old dredge track in the GSR area, small furrows occur at the disturbed sediment surface, most likely caused by the shape of the dredge (Fig. 2).

3.2 Sediment porosity and solid-phase composition

The sediment porosity shows little lateral variability and ranges between 0.65 and 0.8 throughout the upper 25 cm of the sediments at all investigated disturbed sites (Fig. 3). At the disturbed IOM-BIE site, sediment porosity is about 5 % higher in the upper 4 cm of the sediments than below. Bulk Mn contents in the upper 25 cm of the sediments at the disturbed sites are between 0.1 and 0.9 wt % (Fig. 3). Solid-phase Mn contents decrease with depth at all investigated sites. Total organic carbon (TOC) contents in the upper 25 cm of the sediments at the disturbed sites are within 0.2 wt % and 0.5 wt % (Fig. 3). The TOC contents slightly decrease with depth at all investigated sites.

3.3 Pearson correlation coefficient and disturbance depths

The Pearson correlation coefficient r_{Mn} for the correlation of solid-phase Mn contents between the disturbed sites and the respective reference sites ranges between 0.72 and 0.97 (Table 3). Based on r_{Mn} , 5–15 cm of sediment was removed by various disturbance experiments in the different contract areas (Fig. 4). Applying these r_{Mn} -derived disturbance depths for the correlation of the TOC depth distributions between disturbed sites and respective adjacent reference sites gives Pearson correlation coefficients r_{TOC} within 0.73 and 0.91 (Table 3; Fig. 4), which may support the estimates for the disturbance depth based on r_{Mn} . At the BGR-RA site, the correlation of TOC contents between the disturbed site and the reference site shows negative values. As the sediment porosity

in the disturbed sediments correlates well with the porosity in the respective undisturbed reference sediments (Fig. 4), sediment compaction due to the weight of the disturbance device may be negligible during the small-scale disturbances investigated in the framework of this study.

3.4 Transport-reaction modeling

The removal of the surface sediments in the transient transport-reaction model for the BGR-RA and IOM-BIE sites is associated with the loss of the reactive labile organic matter (Figs. 5 and 6). About 10 kyr after the removal of the upper 10 cm of the sediments in the model for the BGR-RA site, oxygen penetrates about 10-fold deeper into the disturbed sediments than in undisturbed sediments (Table 2; Fig. 5; Volz et al., 2018). At the IOM-BIE site, oxygen reaches the maximum OPD at about 100 years after the removal of the upper 7 cm of the sediments. At this site, the oxygen front migrates only ~ 1 m deeper than the corresponding OPD in undisturbed sediments (Table 2; Fig. 5; Volz et al., 2018). As a consequence of deeper OPDs at both sites, the oxic–suboxic redox boundary is located at greater depth, with a significant consumption of pore-water Mn^{2+} in the path of the oxygen front. The NH_4^+ concentrations are also being diminished, reaching minima within 100–1000 years and 1–10 years after the disturbance experiments in the BGR-RA and IOM areas, respectively. The trend for the NO_3^- is more complicated, with lower concentrations during the downward migration of the OPD and augmented concentrations once oxygen concentrations reach their maximum (Figs. 5 and 6).

Naturally, the solute fluxes across the SWI are strongly affected after the surface sediment removal (Fig. 7). The transient transport-reaction model suggests that the oxygen fluxes into the sediments are lowered by a factor of 3–6 after 10–100 years at the IOM-BIE and BGR-RA sites, respectively. This trend is mirrored by the decreased release of NH_4^+ and NO_3^- into the bottom water.

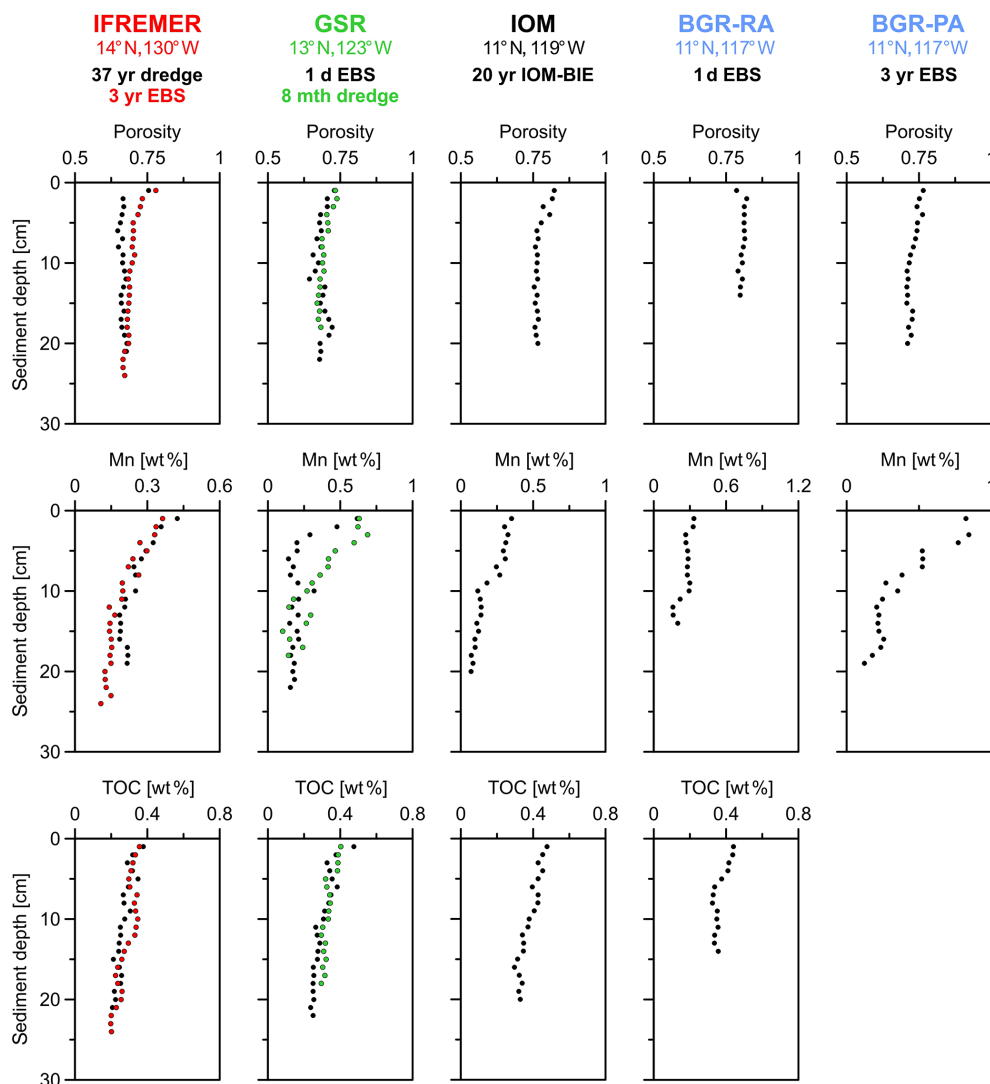


Figure 3. Solid-phase Mn and TOC contents for all disturbed sites investigated in the framework of this study (years: yr; months: mth; days: d).

4 Discussion

4.1 Depths of small-scale disturbance experiments

Our work demonstrates that the depth distribution of solid-phase Mn provides a reliable tool for the determination of the disturbance depths in the sediments of the CCZ (Fig. 4; Table 3). The success of the correlation of solid-phase Mn contents between disturbed and undisturbed reference sediments benefits from several factors.

1. Sediment mixing during the small-scale disturbance experiments is negligible: the visual impact assessment of the investigated disturbance tracks in the CCZ suggests that sediment mixing during the small-scale disturbance experiments was insignificant (Fig. 2). This observation is in agreement with a recent EBS disturbance experi-

ment, which was conducted in the DISCOL area in the Peru Basin in 2015 (Greinert, 2015). The freshly created EBS track in the DISCOL area was revisited 5 weeks after the disturbance experiment, where the surface sediment was mostly removed and deeper sediment layers were exposed without visible sediment mixing (Boetius, 2015; Paul et al., 2018). In a study on the geochemical regeneration in disturbed sediments of the DISCOL area, Paul et al. (2018) have shown that the bulk Mn-rich top sediment layer, which has been observed in undisturbed sediments, is removed in the 5-week old EBS disturbance track. Thus, an important prerequisite for this method is met, and the authors have proposed that the depth distribution of solid-phase Mn may be suitable for the evaluation of the impact as well as for the

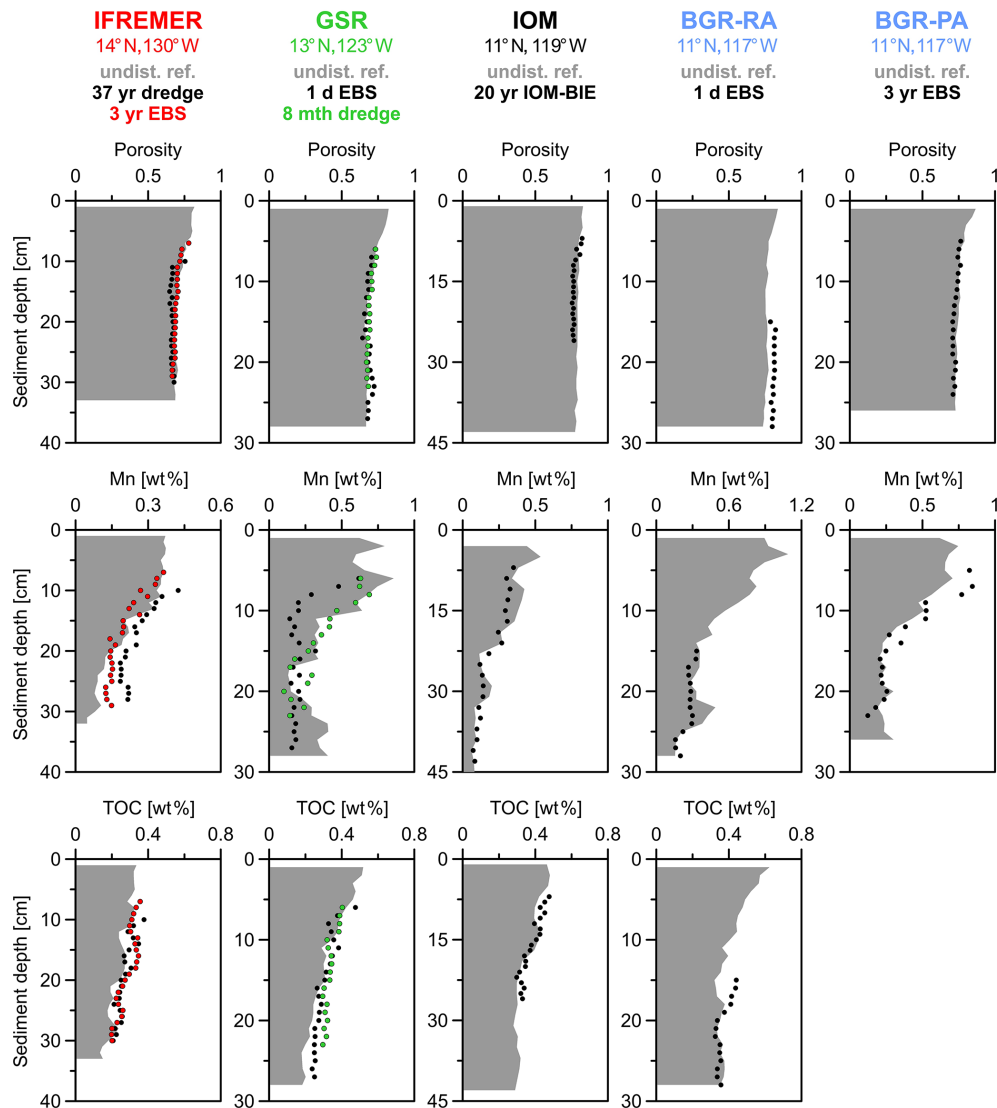


Figure 4. Correlation of solid-phase Mn and TOC contents between the disturbed sites and the respective undisturbed reference sediments (grey shaded profiles) using the disturbance depths determined with the Pearson correlation coefficient (compare Table 3). For the undisturbed reference sediments, solid-phase Mn contents are taken from Volz et al. (2020) and TOC contents are taken from Volz et al. (2018; years: yr; months: mth; days: d).

monitoring of the recovery of small-scale disturbance experiments.

2. The solid-phase Mn maxima in the surface sediments appear to be a regional phenomenon across the CCZ area as has been observed throughout the different exploration areas studied in the framework of this study (Volz et al., 2020): the investigated disturbed sediments as well as the undisturbed reference sediments in the CCZ show decreasing solid-phase Mn contents with depth in the upper 20–30 cm of the sediments (Figs. 3; 4; Volz et al., 2020). In the undisturbed reference sediments, solid-phase Mn contents show maxima of up to 1 wt% in the upper 10 cm of the sediments, with dis-

tinctly decreasing contents below this level (Fig. 4; Volz et al., 2020). Similar bulk solid-phase Mn distribution patterns have been reported for other sites within the CCZ (e.g., Khripounoff et al., 2006; Mewes et al., 2014; Widmann et al., 2015). Volz et al. (2020) have suggested that the widely observed solid-phase Mn enrichments in CCZ surface sediments formed in association with a more compressed oxic zone, which may have prevailed as a result of lower bottom-water oxygen concentrations during the last glacial period than today. Strong indication for lower glacial bottom-water oxygen concentrations throughout the eastern Pacific Ocean have been provided by a number of independent proxies (e.g., An-

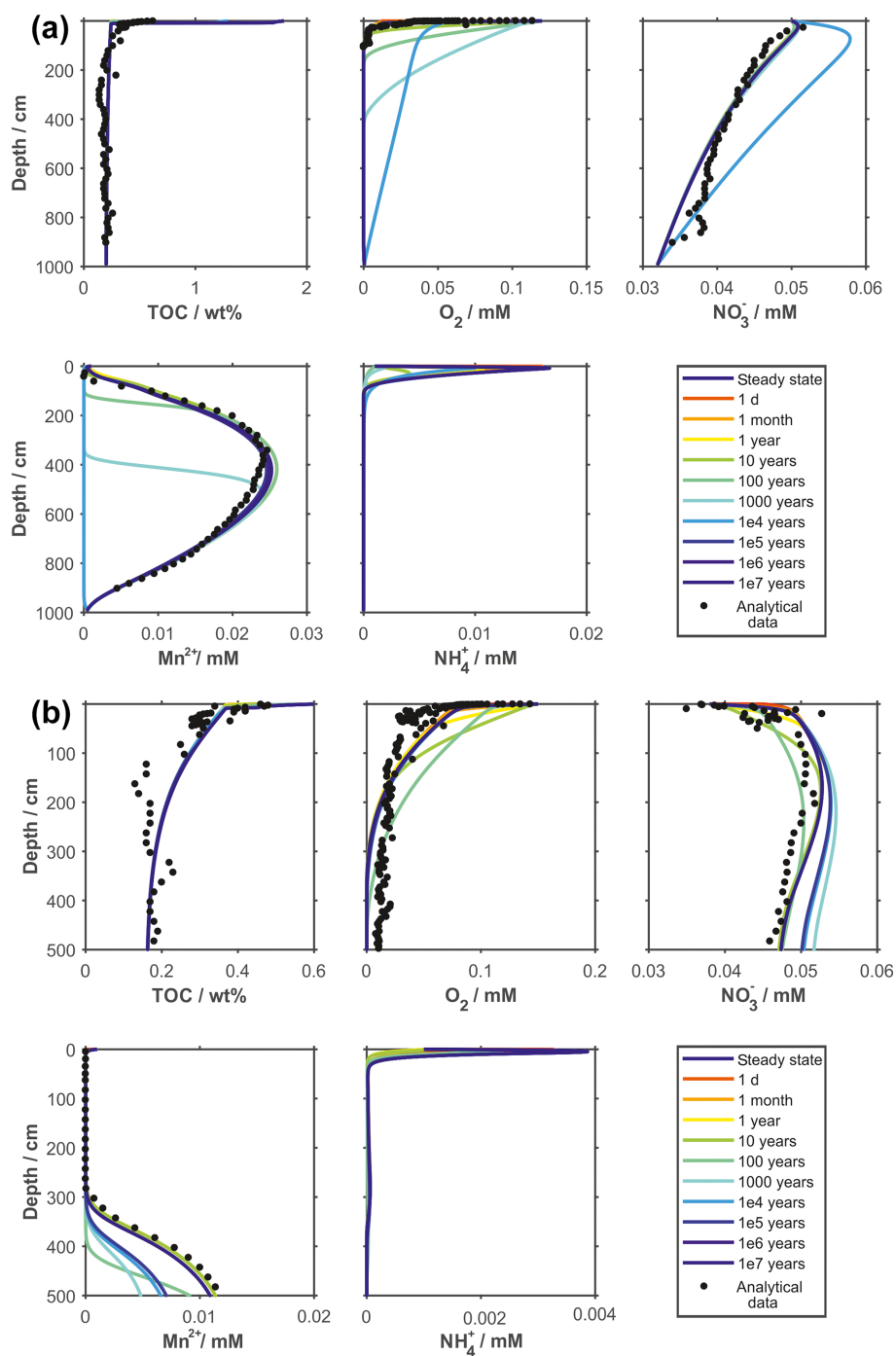


Figure 5. Model results of the transient transport-reaction model showing depth profiles of TOC, O_2 , NO_3^- , Mn^{2+} and NH_4^+ for (a) the EBS disturbance in the German BGR-RA area and (b) the IOM-BIE disturbance in the eastern European IOM area. The model is adapted after the steady-state transport-reaction model presented in Volz et al. (2018) and shows the response of the geochemical system in the sediments if steady-state conditions are disturbed by the removal of the upper 10 cm (BGR-RA; average disturbance depth of BGR-PA and BGR-RA; see Table 3) and 7 cm (IOM; see Table 3) of the sediments while maintaining the same boundary conditions but with reduced bioturbation over the first 100 years after the disturbance.

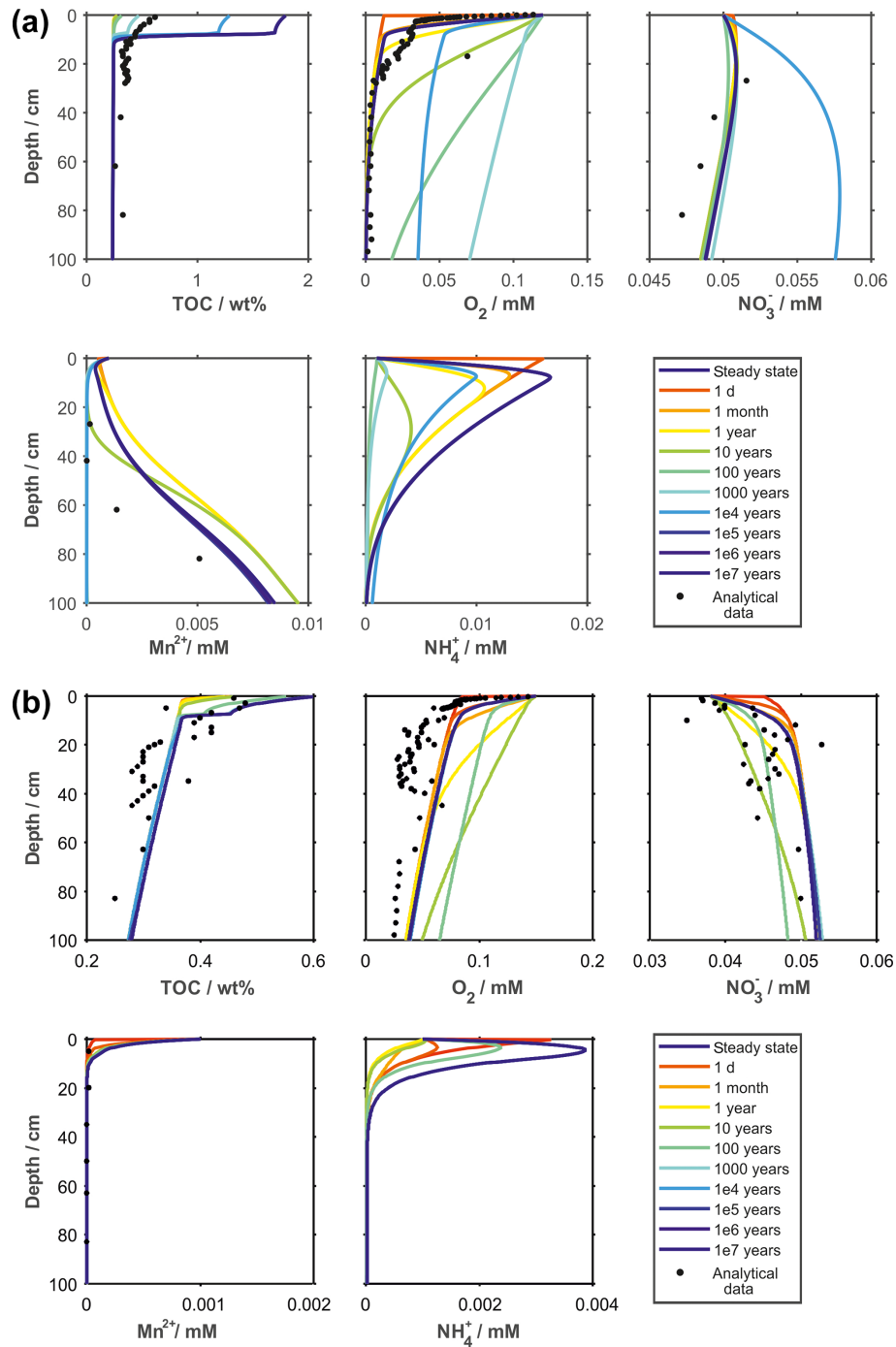


Figure 6. Detailed model results of the transient transport-reaction model (Fig. 5) showing depth profiles of TOC, O_2 , NO_3^- , Mn^{2+} and NH_4^+ for the upper 1 m of the sediments with the fit of the simulated profiles with the analytical data for undisturbed sediments at current steady-state geochemical conditions and for the new steady-state geochemical system after the disturbance (dark blue profiles) for (a) EBS disturbance in the German BGR-RA area and (b) the IOM-BIE disturbance in the eastern European IOM area.

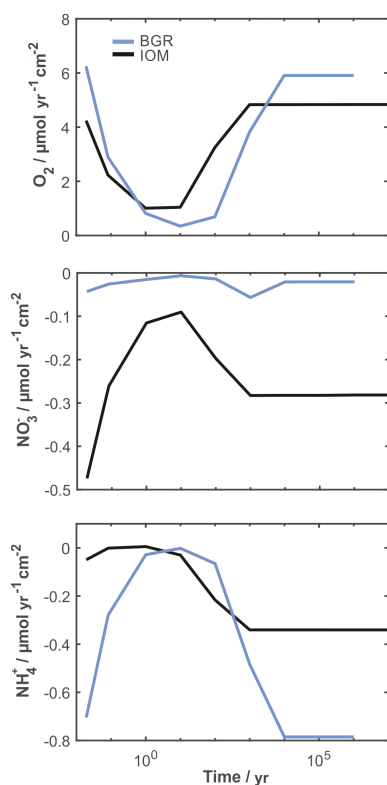


Figure 7. Pore-water fluxes of oxygen (O_2), nitrate (NO_3^-) and ammonia (NH_4^+) at the sediment–water interface obtained by the application of the transient transport–reaction model. Oxygen fluxes into the sediment and fluxes of nitrate and ammonia towards the sediment surface are shown as a function of time after the EBS and IOM-BIE disturbances in the German BGR-RA area (blue) and in the eastern European IOM area (black), respectively.

derson et al., 2019, and references therein). As a consequence of the condensed oxic zone, upwardly diffusing pore-water Mn^{2+} may have precipitated as authigenic Mn(IV) at a shallow oxic–suboxic redox boundary in the upper few centimeters of the sediments. After the last glacial period, the authigenic Mn(IV) peak was continuously mixed into subsequently deposited sediments by bioturbation, causing the observed broad solid-phase Mn(IV) enrichment in the surface sediments (Fig. 4; Volz et al., 2020).

3. Lastly, the OPD at all sites is located at sediment depths greater than 0.5 m, and, thus, diagenetic precipitation of Mn(IV) in the surface sediments (e.g., Gingele and Kastan, 1994) since the last glacial period can be ruled out (Table 2; Mewes et al., 2014; Volz et al., 2020).

Based on the depth distribution of solid-phase Mn, our work suggests that between 5 and 15 cm of the surface sediments was removed and pushed aside by the different small-scale disturbance experiments in the CCZ (Table 3; Fig. 4). This range of disturbance depths is in good agreement with

other estimates for small-scale disturbances by similar gear in the CCZ and in the DISCOL area, which suggest that the upper 4–20 cm of the sediments was removed (e.g., Thiel and Forschungsverband Tiefsee-Umweltschutz, 2001; Oebius et al., 2001; König et al., 2001; Grupe et al., 2001; Radziejewska, 2002; Khripounoff et al., 2006; Paul et al., 2018). However, as the disturbed sites investigated in this study and the respective undisturbed reference sites are located up to 5 km apart from each other, the correlation of solid-phase Mn may be influenced by some spatial heterogeneities in solid-phase Mn contents (Table 1; Mewes et al., 2014). Furthermore, it should be noted that for the correlation of solid-phase Mn contents between the disturbed and undisturbed reference sites, we did not consider that (1) particles may have re-settled on the freshly exposed sediment surfaces from re-suspended particle plumes (e.g., Jankowski and Zielke, 2001; Thiel and Forschungsverband Tiefsee-Umweltschutz, 2001; Radziejewska, 2002; Gillard et al., 2019), (2) sediment slid off from adjacent flanks of the sediment accumulation after the disturbances (Fig. 2), and (3) sediments were deposited after the small-scale disturbances at sedimentation rates between 0.2 and 1.2 cm kyr^{-1} (Table 2; Volz et al., 2018). However, only in the case of the IOM-BIE disturbance, the visual impact assessment suggested that the disturbance surface was concealed, here by re-settling sediments (Fig. 2). The development of a re-suspended particle plume during the disturbance experiments highly depends on various factors, such as sediment properties, seafloor topography, bottom-water currents and the disturbance device (e.g., Gillard et al., 2019). Although local and regional variations in these factors have been reported for the CCZ, they are not well constrained (e.g., Mewes et al., 2014; Aleynik et al., 2017; Volz et al., 2018; Gillard et al., 2019; Hauquier et al., 2019). As the disturbance tracks investigated in the framework of this study are relatively small, with a maximum width of 2.5 m (Fig. 2; Brockett and Richards, 1994; Brenke, 2005), re-suspended particles may (1) only partly deposit on the disturbance track and (2) mostly be transported laterally by currents and deposit on top of undisturbed sediments in the proximity of the disturbance tracks (e.g., Fukushima, 1995; Aleynik et al., 2017; Gillard et al., 2019). This is in accordance with the close correlation of the sediment porosity between the disturbed and undisturbed reference sites, which indicates that the deposition of re-settling particles with higher porosity at the sediment surface in the disturbance tracks is insignificant at all sites, except for the IOM-BIE site (Fig. 4). The porosity data further show that sediment compaction, potentially caused by the weight of the disturbance device (Cuvelier et al., 2018; Hauquier et al., 2019), is insignificant at all disturbed sites.

4.2 Impact of small-scale disturbances on the geochemical system

The geochemical conditions found at the study sites in the CCZ are the result of a balanced interplay of key factors, such as the input of fresh, labile TOC, sedimentation rate and bioturbation intensity (e.g., Froelich et al., 1979; Berner, 1981; Zonneveld et al., 2010; Mogollón et al., 2016; Volz et al., 2018). Together they characterize the upper reactive layer, which in turn plays a crucial role in the location of the OPD in the sediments of the CCZ (e.g., Mewes et al., 2014; Mogollón et al., 2016; Volz et al., 2018). Oxygen is consumed via aerobic respiration during the degradation of organic matter, while bioturbation transports fresh, labile TOC into deeper sediments (e.g., Haeckel et al., 2001; König et al., 2001). The presence of labile TOC throughout the bioturbated zone significantly enhances the consumption of oxygen with depth, where oxygen is not as easily replenished by seawater oxygen. Thus, the availability of labile TOC in the bioturbated layer controls the amount of oxygen that passes through the reactive layer into deeper sediments (e.g., König et al., 2001). Below the highly reactive layer, refractory organic matter degradation and secondary redox reactions – such as oxidation of Mn^{2+} – control the consumption of oxygen (Table S1; Mogollón et al., 2016; Volz et al., 2018). The oxygen profile, more precisely the position of the OPD, in turn, strongly influences the distribution of other solutes. Below the OPD, denitrification and Mn(IV) reduction commence, albeit at much lower rates, consuming pore-water NO_3^- and releasing Mn^{2+} (Mogollón et al., 2016; Volz et al., 2018). The study sites in the CCZ provide an excellent example for how slight differences in key environmental factors can profoundly change the overall solute profiles, with OPDs ranging between 0.5 m (BGR-RA) and > 7.4 m (GSR), as outlined by Volz et al. (2018).

The removal of the upper 5–15 cm of the sediment results, on one hand, in an almost complete loss of the labile TOC fraction (Fig. 4), as this fraction is restricted to the upper 20 cm of the sediment in the CCZ (e.g., Müller and Mangini, 1980; Emerson, 1985; Müller et al., 1988; Mewes et al., 2014; Mogollón et al., 2016; Volz et al., 2018). On the other hand, studies on faunal diversity and density in small-scale disturbances in the sediments of the CCZ and in the DISCOL area show that most of the biota is lost immediately after the disturbance experiment (Borowski and Thiel, 1998; 2001; Bluhm et al., 2001; Thiel et al., 2001; Vanreusel et al., 2016; Jones et al., 2017; Gollner et al., 2017). Thus, a drastic decline or standstill of bioturbation can be expected in the surface sediments.

Based on the results of the transient transport-reaction model, geochemical recovery after small-scale sediment disturbances can be divided into two main phases (Fig. 8).

1. Since the labile TOC fraction and bioturbating fauna are mostly removed, downward diffusion of oxygen is the

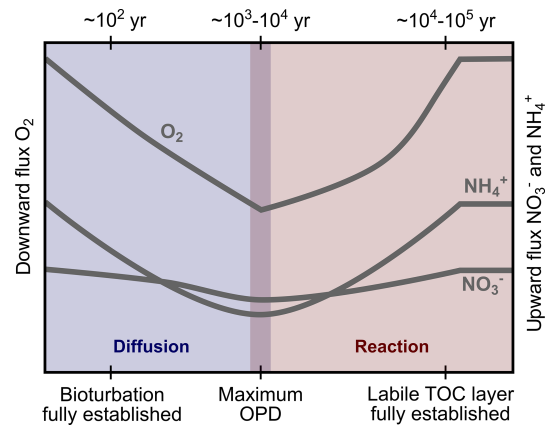


Figure 8. Conceptual model for time-dependent pore-water fluxes of oxygen (O_2), nitrate (NO_3^-) and ammonia (NH_4^+) at the sediment–water interface after the removal of the upper 7–10 cm of the sediments. The re-establishment of bioturbation, the maximum oxygen penetration depth (OPD) and the re-establishment of the surface sediment layer dominated by the reactive labile organic matter fraction are indicated as a function of time after the sediment removal (years: yr).

main driver shaping solute profiles towards a new geochemical steady-state system in the absence of the reactive layer (Figs. 5 and 6). This entails the downward migration of the OPD, as oxygen is no longer effectively consumed in the upper sediment layer. The presence of oxygen outcompetes denitrification and Mn(IV) reduction and induces NH_4^+ and Mn^{2+} oxidation instead, thus minimizing pore-water NH_4^+ and Mn^{2+} concentrations (Figs. 5 and 6). At the same time, NO_3^- , produced during nitrification in the presence of oxygen (e.g., Froelich et al., 1979; Berner, 1981; Haeckel et al., 2001; Mogollón et al., 2016; Volz et al., 2018), is accordingly reduced during denitrification, and NO_3^- concentrations are lowered during this first phase.

2. The second phase is characterized by the increasing influence of reactive fluxes across the seafloor. It takes approximately 1000 years before any significant build-up of an upper labile TOC layer is re-established (Fig. 6), at which point solute profiles slowly shift towards their pre-disturbance shape (Fig. 7). Interestingly, during the transition time, when oxygen is still present at depth but aerobic respiration in the upper sediments has already begun to pick up, NO_3^- concentrations are strongly elevated in the BGR sediments (Figs. 5 and 6). This is due to the fact that NO_3^- is not consumed during denitrification or the Mn–anammox reaction in the presence of oxygen (Mogollón et al., 2016; Volz et al., 2018).

With the importance of bioturbation and the mining-related removal of associated fauna in mind, solute and in particular nutrient fluxes across the seafloor should also be

considered. The release of nutrients complements the close link between sediment geochemistry and the food web structure (e.g., Smith et al., 1979; Dunlop et al., 2016; Stratmann et al., 2018) and further emphasizes their interdependencies. Figure 7 depicts fluxes of oxygen, NO_3^- and NH_4^+ across the seafloor. As expected, with the reactive layer being mostly absent, fluxes across the seafloor are severely reduced, which particularly affects the oxygen uptake of the sediments as well as the release of NO_3^- and NH_4^+ into the bottom water. At about 100 to 1000 years after the disturbance, concurrent with the build-up of an upper sediment layer containing significant amounts of labile organic matter, fluxes begin to increase again, albeit much slower than the rate of the decrease in fluxes subsequently after the disturbances (Fig. 7; note the logarithmic scale).

It should be noted that while bioturbation has a pivotal influence on the undisturbed steady-state profile, it only plays a secondary role in re-establishing the steady-state geochemical system at the disturbed sites in the CCZ. Studies suggest that faunal abundances fully recover within centuries after the disturbance even though the benthic community may be different than prior to the disturbance (e.g., Miljutin et al., 2011; Vanreusel et al., 2016). Due to the extremely slow build-up of the reactive layer with labile TOC, the bioturbation “pump” is active again before any significant amount of labile TOC is present about 1–100 kyr after the disturbance. Thus, full recovery is mainly controlled by the re-establishment of the upper reactive layer, i.e., the delivery rate of labile TOC to the seafloor.

The transport-reaction model reveals that under current depositional conditions, the new steady-state geochemical system is established after 1–10 kyr at the IOM-BIE site, while the re-establishment of steady-state geochemical conditions at the BGR-RA site takes 10–100 kyr (Figs. 5 and 6). Shorter recovery times at the IOM site compared to the BGR-RA site are related to higher sedimentation rates (1.15 instead of 0.65 cm kyr^{-1}) and shallower impact on the sediment (7 cm instead of 10 cm sediment removal). Accordingly, the maximum OPD is reached after 100 years and 10 kyr at the IOM and BGR-RA site, respectively (Figs. 5 and 6), while the reactive layer is clearly established sooner at the IOM site compared to the BGR-RA site (Fig. 7). Thus, the disturbance depth clearly has a strong influence on the recovery process of the geochemical system of the sediments, highlighting the importance of low-impact mining equipment. Considering that in the CCZ areas of about 8500 km^2 could be commercially mined in 20 years per individual mining operation (Madureira et al., 2016), this impact assessment of small-scale disturbance experiments may only represent a first approach for the prediction of the environmental impact of large-scale deep-sea mining activities.

5 Conclusion

We studied surface sediments from seven small-scale disturbance experiments for the simulation of deep-sea mining, which were performed between 1 d and 37 years prior to our sampling in the NE Pacific Ocean. These small-scale disturbance tracks were created using various disturbance devices in different European contract areas for the exploration of polymetallic nodules within the eastern part of the Clarion–Clipperton Zone (CCZ). Through correlation of solid-phase Mn contents of disturbed and undisturbed reference sediments, we (1) propose that the depth distribution of solid-phase Mn in the sediments of the CCZ provides a reliable tool for the estimation of the disturbance depth and (2) show that 5–15 cm of the sediments was removed during the small-scale disturbance experiments investigated in this study. As the small-scale disturbances are associated with the removal of the surface sediments characterized by reactive labile organic matter, the disturbance depth ultimately determines the impact on the geochemical system in the sediments. The application of a transient transport-reaction model reveals that the removal of the upper 7–10 cm of the surface sediments is associated with a meter-scale downward extension of the oxic zone and the shutdown of denitrification and Mn(IV) reduction. As a consequence of lower respiration rates after the disturbance experiments, the geochemical system in the sediments is controlled by downward oxygen diffusion. While the re-establishment of bioturbation within centuries after the disturbance is important for the development of steady-state geochemical conditions in the disturbed sediments, the rate at which geochemical steady-state conditions are reached ultimately depends on the delivery rate of organic matter to the seafloor. Assuming the accumulation of labile organic matter to proceed at current Holocene sedimentation rates in the disturbed sediments, biogeochemical reactions resume in the reactive surface sediment layer, and, thus, the new steady-state geochemical system in the disturbed sediments in the CCZ is reached on a millennial timescale after the disturbance of the surface sediments.

Our study represents the first study on the impact of small-scale disturbance experiments on the sedimentary geochemical system in the prospective areas for polymetallic nodule mining in the CCZ. Our findings on the evaluation of the disturbance depths using solid-phase Mn contents as well as the quantification of the development of a new geochemical steady-state system in the sediments advance our knowledge about the potential long-term consequences of deep-sea mining activities. We propose that mining techniques potentially used for the potential commercial exploitation of nodules in the CCZ may remove less than 10 cm of the surface sediments in order to minimize the impact on the geochemical system in the sediments. The depth distribution of solid-phase Mn may be used for environmental monitoring purposes during future mining activities in the CCZ. However, based on our current knowledge and in combination

with ongoing natural environmental changes (e.g., bottom-water warming, acidification, changes in the POC flux to the seafloor), it is difficult to assess whether the surface sediment removal may trigger a tipping point for deep-sea ecosystems. This study also provides valuable data for further investigations on the environmental impact of deep-sea mining, such as during the launched JPI Oceans follow-up project MiningImpact 2.

Data availability. The data are available via the data management portal OSIS-Kiel and the WDC database PANGAEA, including the solid-phase bulk sediment Mn and TOC contents (<https://doi.org/10.1594/PANGAEA.904560>; Volz et al., 2019a) as well as the porosity data (<https://doi.org/10.1594/PANGAEA.904578>; Volz et al., 2019b).

Supplement. The supplement related to this article is available online at: <https://doi.org/10.5194/bg-17-1113-2020-supplement>.

Author contributions. The study was conceived by all co-authors. JBV carried out the sampling and analyses onboard during the RV SONNE cruise SO239 and the analytical work in the laboratories at the Alfred Wegener Institute (AWI) in Bremerhaven. LH and MH modified the numerical transport-reaction model presented in Volz et al. (2018) and provided model results for the long-term effects of small-scale disturbances on geochemical conditions and biogeochemical processes. JBV prepared the paper, with substantial contributions from all co-authors.

Competing interests. The authors declare that they have no conflict of interest.

Special issue statement. This article is part of the special issue “Assessing environmental impacts of deep-sea mining – revisiting decade-old benthic disturbances in Pacific nodule areas”. It is not associated with a conference.

Acknowledgements. We thank captain Lutz Mallon, the crew and the scientific party of RV SONNE cruise SO239 for the technical and scientific support. Thanks to Jennifer Ciomber, Benjamin Löffler and Vincent Ozegowski for their participation in sampling and analysis onboard. For analytical support in the home laboratory and during data evaluation we are grateful to Ingrid Stimac, Olaf Kreft, Dennis Köhler and Ingrid Dohrmann (all at AWI). We especially thank Gerhard Bohrmann (MARUM, University of Bremen), Timothy G. Ferdeman (MPI Bremen) and Ellen Pape (University of Ghent) for much appreciated discussions. We thank Jack Middelburg and the two anonymous referees for editing and reviewing this paper.

Financial support. This research was funded by the Bundesministerium für Bildung und Forschung (grant no. 03F0707A+G) as part of the JPI Oceans pilot action “Ecological aspects of deep-sea mining (MiningImpact). Further financial support was provided by the Alfred Wegener Institute Helmholtz Centre for Polar and Marine Research.

The article processing charges for this open-access publication were covered by a Research Centre of the Helmholtz Association.

Review statement. This paper was edited by Jack Middelburg and reviewed by two anonymous referees.

References

- Aleynik, D., Inall, M. E., Dale, A., and Vink, A.: Impact of remotely generated eddies on plume dispersion at abyssal mining sites in the Pacific, *Sci. Rep.-UK*, 7, 1–14, <https://doi.org/10.1038/s41598-017-16912-2>, 2017.
- Anderson, R. F., Sachs, J. P., Fleisher, M. Q., Allen, K. A., Yu, J., Koutavas, A., and Jaccard, S. L.: Deep-sea oxygen depletion and ocean carbon sequestration during the last ice age, *Global Biogeochem. Cy.*, 33, 301–317, <https://doi.org/10.1029/2018GB006049>, 2019.
- Berger, W. H.: Deep-sea sedimentation, in: *The Geology of Continental Margins*, edited by: Burk, C. A. and Drake, C. L., Springer, New York, 213–241, 1974.
- Berner, R. A.: *Early Diagenesis: A Theoretical Approach*, Princeton University Press, Princeton, 1–24, 1980.
- Berner, R. A.: A new geochemical classification of sedimentary environments, *J. Sediment. Petrol.*, 51, 359–365, 1981.
- Bluhm H.: Re-establishment of an abyssal megabenthic community after experimental physical disturbance of the seafloor, *Deep-Sea Res. Pt. II*, 48, 3841–3868, 2001.
- Boetius, A.: RV SONNE Fahrtbericht/Cruise Report SO242-2: JPI OCEANS Ecological Aspects of Deep-Sea Mining, DISCOL Revisited, Guayaquil-Guayaquil (Equador), 28 August–1 October 2015, GEOMAR Helmholtz-Zentrum für Ozeanforschung, Kiel, 2015.
- Boetius, A. and Haeckel, M.: Mind the seafloor, *Science*, 359, 34–36, <https://doi.org/10.1126/science.aap7301>, 2018.
- Borowski, C. and Thiel, H.: Deep-Sea macrofaunal impacts of a large-scale physical disturbance experiment in the Southeast Pacific, *Deep-Sea Res. Pt. II*, 45, 55–81, 1998.
- Boudreau, B. P.: A one-dimensional model for bed-boundary layer particle exchange, *J. Marine Syst.*, 11, 279–303, [https://doi.org/10.1016/S0924-7963\(96\)00127-3](https://doi.org/10.1016/S0924-7963(96)00127-3), 1997.
- Brenke, N.: An Epibenthic sledge for operations on marine soft bottom and bedrock, *J. Mar. Tech. Soc.*, 39, 10–19, 2005.
- Brockett, T. and Richards, C. Z.: Deep-sea mining simulator for environmental impact studies, *Sea Technol.*, 35, 77–82, 1994.
- Chung, J. S.: Full-Scale, Coupled Ship and Pipe Motions Measured in North Pacific Ocean: The Hughes Glomar Explorer with a 5,000-m-Long Heavy-Lift Pipe Deployed, *Proc. 19th ISOPE*, 20, 1–6, 2010.

- Cronan, D. S., Rothwell, G., and Croudace, I.: An ITRAX geochemical study of ferromanganiferous sediments from the Penrhyn basin, South Pacific Ocean, *Mar. Georesour. Geotec.*, 28, 207–221, <https://doi.org/10.1080/1064119X.2010.483001>, 2010.
- Cuvelier, D., Gollner, S., Jones, D. O. B., Kaiser, S., Arbizu, P. M., Menzel, L., Mestre, N. C., Morato, T., Pham, C., Pradillon, F., Purser, A., Raschka, U., Sarrazin, J., Simon-Lledó, E., Stewart, I. M., Stuckas, H., Sweetman, A. K., and Colaço, A.: Potential Mitigation and Restoration Actions in Ecosystems Impacted by Seabed Mining, *Front. Mar. Sci.*, 5, 467, <https://doi.org/10.3389/fmars.2018.00467>, 2018.
- Davies, A. J., Roberts, J. M., and Hall-Spencer, J.: Preserving deep-sea natural heritage: emerging issues in offshore conservation and management, *Biol. Conserv.*, 138, 299–312, <https://doi.org/10.1016/j.biocon.2007.05.011>, 2007.
- Dunlop, K. M., van Oevelen, D., Ruhl, H. A., Huffard, C. L., Kuhn, L. A., and Smith, K. L.: Carbon cycling in the deep eastern North Pacific benthic food web: Investigating the effect of organic carbon input, *Limnol. Oceanogr.*, 61, 1956–1968, <https://doi.org/10.1002/lno.10345>, 2016.
- Emerson, S., Fischer, K., Reimers, C., and Heggie, D.: Organic carbon dynamics and preservation in deep-sea sediments, *Deep-Sea Res.*, 32, 1–21, 1985.
- Froelich, P. N., Klinkhammer, G. P., Bender, M. L., Luedke, L. A., Heath, G. R., Cullen, C., Dauphin, P., Hammond, D., Hartmann, B., and Maynard, V.: Early oxidation of organic matter in pelagic sediments of the Eastern Equatorial Pacific, suboxic diagenesis, *Geochim. Cosmochim. Ac.*, 43, 1075–1090, 1979.
- Fukushima, T.: Overview “Japan Deep-Sea Impact Experiment = JET”, *Proc. 1st ISOPE*, 47–53, ISOPE-M-95-008, 1995.
- Gillard, B., Purkiani, K., Chatzievangelou, D., Vink, A., Iversen, M. H., and Thomsen, L.: Physical and hydrodynamic properties of deep sea mining-generated, abyssal sediment plumes in the Clarion Clipperton Fracture Zone (eastern-central Pacific), *Elem. Sci. Anth.*, 7, 5, <https://doi.org/10.1525/elementa.343>, 2019.
- Gingele, F. X. and Kasten, S.: Solid-phase manganese in Southeast Atlantic sediments: implications for the paleoenvironment, *Mar. Geol.*, 121, 317–332, 1994.
- Glasby, G. P.: Lessons Learned from Deep-Sea Mining, *Science*, 289, 551–553, <https://doi.org/10.1126/science.289.5479.551>, 2000.
- Glover, A. G. and Smith, C. R.: The deep-sea floor ecosystem: current status and prospects of anthropogenic change by the year 2025, *Environ. Conserv.*, 30, 219–241, 2003.
- Gollner, S., Kaiser, S., Menzel, L., Jones, D. O. B., Brown, A., Mestre, N. C., van Oevelen, D., Menot, L., Colaço, A., Canals, M., Cuvelier, D., Durden, J. M., Gebruk, A., Egho, G. A., Haeckel, M., Marcon, Y., Mevenkamp, L., Morato, T., Pham, C. K., Purser, A., Sanchez-Vidal, A., Vanreusel, A., Vink, A., and Arbizu, P. M.: Resilience of benthic deep-sea fauna to mining activities, *Mar. Environ. Res.*, 129, 76–101, <https://doi.org/10.1016/j.marenvres.2017.04.010>, 2017.
- Greinert, J.: RV SONNE Fahrtbericht/Cruise Report SO242-1: JPI OCEANS Ecological Aspects of Deep-Sea Mining, DISCOL Revisited, Guayaquil-Guayaquil (Ecuador), 28 July–25 August 2015, GEOMAR Helmholtz-Zentrum für Ozeanforschung, Kiel, 2015.
- Grupe, B., Becker, H. J., and Oebius, H. U.: Geotechnical and sedimentological investigations of deep-sea sediments from a manganese nodule field of the Peru Basin, *Deep-Sea Res. Pt. II*, 48, 3593–3608, 2001.
- Haeckel, M., König, I., Riech, V., Weber, M. E., and Suess, E.: Pore water profiles and numerical modelling of biogeochemical processes in Peru Basin deep-sea sediments, *Deep-Sea Res. Pt. II*, 48, 3713–3736, [https://doi.org/10.1016/S0967-0645\(01\)00064-9](https://doi.org/10.1016/S0967-0645(01)00064-9), 2001.
- Halbach, P., Friedrich, G., and von Stackelberg, U. (Eds.): The manganese nodule belt of the Pacific Ocean, Enke, Stuttgart, 1988.
- Halfar, J. and Fujita, R. M.: Precautionary management of deep-sea mining, *Mar. Policy*, 26, 103–106, 2002.
- Halkyard, J. E.: Technology for Mining Cobalt Rich Manganese Crusts from Seamounts, *Proc. OCEANS*, Proc. OCEANS, 12 November–14 November 1985, San Diego, CA, USA, 352–274, 1985.
- Hauquier, F., Macheriotou, L., Bezerra, T. N., Egho, G., Martínez Arbizu, P., and Vanreusel, A.: Distribution of free-living marine nematodes in the Clarion–Clipperton Zone: implications for future deep-sea mining scenarios, *Biogeosciences*, 16, 3475–3489, <https://doi.org/10.5194/bg-16-3475-2019>, 2019.
- Hein, J. R., Mizell, K., Koschinsky, A., and Conrad, T. A.: Deep-ocean mineral deposits as a source of critical metals for high- and green-technology applications: comparison with land-based resources, *Ore Geol. Rev.*, 51, 1–14, 2013.
- Hoagland, P., Beaulieu, S., Tivey, M. A., Eggert, R. G., German, C., Glowka, L., and Lin, J.: Deep-sea mining of seafloor massive sulfides, *Mar. Policy*, 34, 728–732, <https://doi.org/10.1016/j.marpol.2009.12.001>, 2010.
- International Seabed Authority (ISA): A Geological Model for Polymetallic Nodule Deposits in the Clarion–Clipperton Fracture Zone, Technical Study 6, Kingston, p. 211, 2010.
- Jankowski, J. A. and Zielke, W.: The mesoscale sediment transport due to technical activities in the deep sea, *Deep-Sea Res. Pt. II*, 48, 3487–3521, 2001.
- Jones, D. O. B., Kaiser, S., Sweetman, A. K., Smith, C. R., Menot, L., Vink, A., Trueblood, D., Greinert, J., Billett, D. S. M., Martínez Arbizu, P., Radziejewska, T., Singh, R., Ingle, B., Stratmann, T., Simon-Lledó, E., Durden, J. M., and Clark, M. R.: Biological responses to disturbance from simulated deep-sea polymetallic nodule mining, *PLoS One*, 12, e0171750, <https://doi.org/10.1371/journal.pone.0171750>, 2017.
- Juan, C., Van Rooij, D., and De Bruycker, W.: An assessment of bottom current controlled sedimentation in Pacific Ocean abyssal environments, *Mar. Geol.*, 403, 20–33, 2018.
- Khripounoff, A., Caprais, J.-C., Crassous, P., and Etoubleau, J.: Geochemical and biological recovery of the disturbed seafloor in polymetallic nodule fields of the Clipperton–Clarion Fracture Zone (CCFZ) at 5,000-m depth, *Limnol. Oceanogr.*, 51, 2033–2041, <https://doi.org/10.4319/lno.2006.51.5.2033>, 2006.
- König, I., Haeckel, M., Lougear, A., Suess, E., and Trautwein, A. X.: A geochemical model of the Peru Basin deep-sea floor – and the response of the system to technical impacts, *Deep-Sea Res. Pt. II*, 48, 3737–3756, [https://doi.org/10.1016/S0967-0645\(01\)00065-0](https://doi.org/10.1016/S0967-0645(01)00065-0), 2001.
- Kotlinski, R. and Stoyanova V.: Physical, Chemical, and Geological changes of Marine Environment Caused by the Benthic Impact Experiment at the IOM BIE Site, *Proc. 8th ISOPE 2*, 277–281, Montreal, Canada, 1998.

- Kretschmer, S., Geibert, W., Rutgers van der Loeff, M. M., and Mollenhauer, G.: Grain size effects on $^{230}\text{Th}_{\text{XS}}$ inventories in opal-rich and carbonate-rich marine sediments, *Earth Planet. Sc. Lett.*, 294, 131–142, <https://doi.org/10.1016/j.epsl.2010.03.021>, 2010.
- Kuhn, G.: Don't forget the salty soup: Calculations for bulk marine geochemistry and radionuclide geochronology, Goldschmidt 2013 Florence, Italy, 25 August 2013–30 August 2013, <https://doi.org/10.1180/minmag.2013.077.5.11>, 2013.
- Kuhn, T., Rühlemann, C., and Wiedicke-Hombach, M.: Developing a strategy for the exploration of vast seafloor areas for prospective manganese nodule fields, in: *Marine Minerals: Finding the Right Balance of Sustainable Development and Environmental Protection*, edited by: Zhou, H. and Morgan, C. L., The Underwater Mining Institute, Gelendzhik, Russia (K 1-12), 2012.
- Kuhn, T., Wegorzewski, A. V., Rühlemann, C., and Vink, A.: Composition, formation, and occurrence of polymetallic nodules, in: *Deep-Sea Mining*, edited by: Sharma, R., 23–63, Springer International Publishing, Cham, https://doi.org/10.1007/978-3-319-52557-0_2, 2017a.
- Kuhn, T., Versteegh, G. J. M., Villinger, H., Dohrmann, I., Heller, C., Koschinsky, A., Kaul, N., Ritter, S., Wegorzewski, A. V., and Kasten, S.: Widespread seawater circulation in 18–22 Ma oceanic crust: Impact on heat flow and sediment geochemistry, *Geology*, 45, 799–802, <https://doi.org/10.1130/G39091.1>, 2017b.
- Lodge, M., Johnson, D., Le Gurun, G., Wengler, M., Weaver, P., and Gunn, V.: Seabed mining: International Seabed Authority environmental management plan for the Clarion–Clipperton Zone. A partnership approach, *Mar. Policy*, 49, 66–72, <https://doi.org/10.1016/j.marpol.2014.04.006>, 2014.
- Madureira, P., Brekke, H., Cherkashov, G., and Rovere, M.: Exploration of polymetallic nodules in the Area: Reporting practices, data management and transparency, *Mar. Policy*, 70, 101–107, <https://doi.org/10.1016/j.marpol.2016.04.051>, 2016.
- Martínez Arbizu, P., and Haeckel, M.: RV *SONNE* Fahrtbericht/Cruise Report SO239: JPI OCEANS Ecological Aspects of Deep-Sea Mining, EcoResponse Assessing the Ecology, Connectivity and Resilience of Polymetallic Nodule Field Systems, Balboa (Panama) – Manzanillo (Mexico.) 11 March–30 April 2015, (Report No. https://doi.org/10.3289/GEOMAR_REP_NS_25_2015), GEOMAR Helmholtz-Zentrum für Ozeanforschung, Kiel, 2015.
- Menendez, A., James, R. H., Lichtschlag, A., Connelly, D., and Peel, K.: Controls on the chemical composition on ferromanganese nodules in the Clarion–Clipperton Fracture Zone, eastern equatorial Pacific, *Mar. Geol.*, 409, 1–14, 2018.
- Menot, L., Rühlemann, C., and BIONOD Shipboard party: BIONOD Cruise Science Report, Vol. 2 French License Area, Ifremer, REM/EEP/LEP13.06, 57 pp., 2013.
- Mero, J. L.: *The Mineral Resources of the Sea*, Elsevier, Amsterdam, 1965.
- Mewes, K., Mogollón, J. M., Picard, A., Rühlemann, C., Kuhn, T., Nöthen, K., and Kasten, S.: Impact of depositional and biogeochemical processes on small scale variations in nodule abundance in the Clarion–Clipperton Fracture Zone, *Deep-Sea Res. Pt. I*, 91, 125–141, <https://doi.org/10.1016/j.dsr.2014.06.001>, 2014.
- Mewes, K., Mogollón, J. M., Picard, A., Rühlemann, C., Eisenhauer, A., Kuhn, T., Ziebis, W., and Kasten, S.: Diffusive transfer of oxygen from seamount basaltic crust into overlying sediments: An example from the Clarion–Clipperton Fracture Zone, *Earth Planet. Sc. Lett.*, 433, 215–225, <https://doi.org/10.1016/j.epsl.2015.10.028>, 2016.
- Miljutin, D. M., Miljutina, M. A., Martínez Arbizu, P., and Galeron, J.: Deep-sea nematode assemblage has not recovered 26 years after experimental mining of polymetallic nodules (CCFZ, Pacific), *Deep-Sea Res. Pt. I*, 58, 885–897, 2011.
- Mogollón, J. M., Mewes, K., and Kasten, S.: Quantifying manganese and nitrogen cycle coupling in manganese-rich, organic carbon-starved marine sediments: Examples from the Clarion–Clipperton fracture zone, *Geophys. Res. Lett.*, 43, GL069117, <https://doi.org/10.1002/2016GL069117>, 2016.
- Morgan, C. L., Nichols, J. A., Selk, B. W., Toth, J. R., and Wallin, C.: Preliminary analysis of exploration data from Pacific deposits of manganese nodules, *Mar. Georesour. Geotec.*, 11, 1–25, 1993.
- Müller, P. J. and Mangini, A.: Organic carbon decomposition rates in sediments of the Pacific manganese nodule belt dated by ^{230}Th and ^{231}Pa , *Earth Planet. Sc. Lett.*, 51, 94–114, 1980.
- Müller, P. J., Hartmann, M., and Suess, E.: The chemical environment of pelagic sediments, in: *The Manganese Nodule Belt of the Pacific Ocean: Geological Environment, Nodule Formation, and Mining Aspects*, edited by: Halbach, P., Friedrich, G., and von Stackelberg, U., Enke, Stuttgart, 70–90, 1988.
- Nöthen, K. and Kasten, S.: Reconstructing changes in seep activity by means of pore water and solid phase Sr/Ca and Mg/Ca ratios in pockmark sediments of the Northern Congo Fan, *Mar. Geol.*, 287, 1–13, <https://doi.org/10.1016/j.margeo.2011.06.008>, 2011.
- Oebius, H. U., Becker, H. J., Rolinski, S., and Jankowski, J. A.: Parametrization and evaluation of marine environmental impacts produced by deep-sea manganese nodule mining, *Deep-Sea Res. Pt. II*, 48, 3453–3467, [https://doi.org/10.1016/S0967-0645\(01\)00052-2](https://doi.org/10.1016/S0967-0645(01)00052-2), 2001.
- Paul, S. A. L., Gaye, B., Haeckel, M., Kasten, S., and Koschinsky, A.: Biogeochemical Regeneration of a Nodule Mining Disturbance Site: Trace Metals, DOC and Amino Acids in Deep-Sea Sediments and Pore Waters, *Front. Mar. Sci.*, 5, 117, <https://doi.org/10.3389/fmars.2018.00117>, 2018.
- Pearson, K.: Notes on regression and inheritance in the case of two parents, *P. Royal Soc. Lond.*, 58, 240–242, 1895.
- Purser, A., Marcon, Y., Hoving, H.-J. T., Vecchione, M., Piatkowski, U., Eason, D., Bluhm, H., and Boetius, A.: Association of deep-sea incirrate octopods with manganese crusts and nodule fields in the Pacific Ocean, *Curr. Biol.*, 26, R1268–R1269, <https://doi.org/10.1016/j.cub.2016.10.052>, 2016, 2016.
- Radziejewska, T.: Response of deep-sea meiobenthic communities to sediment disturbance simulating effects of polymetallic nodule mining, *Int. Rev. Hydrobiol.*, 87, 457–477, 2002.
- Ramirez-Llodra E., Tyler P. A., Baker M. C., Bergstad O. A., Clark M. R., Escobar, E., Levin, L. A., Menot, L., Rowden, A. A., Smith, C. R., and Van Dover, C. L.: Man and the Last Great Wilderness: Human Impact on the Deep Sea, *PLoS ONE*, 6, e22588, <https://doi.org/10.1371/journal.pone.0022588>, 2011.
- Rühlemann, C., Kuhn, T., Wiedicke, M., Kasten, S., Mewes, K., and Picard, A.: Current status of manganese nodule exploration in the German license area, *Proc. 9th ISOPE*, 168–173, 2011.
- Rühlemann, C., Menot, L., and BIONOD Shipboard party: BIONOD Cruise Science Report, Vol. 1 German License Area, BGR, 302 pp., 2013.

- Scott, S. D.: Seafloor Polymetallic Sulfides: Scientific Curiosities or Mines of the Future?, in: *Marine Minerals*, edited by: Teleki, P. G., Dobson, M. R., Moore, J. R., and von Stackelberg, U., NATO ASI Series (Series C: Mathematical and Physical Sciences), 194, Springer, Dordrecht, 1987.
- Sharma, R.: Indian Deep-sea Environment Experiment (IN-DEX): An appraisal, *Deep-Sea Res. Pt. II*, 48, 3295–3307, [https://doi.org/10.1016/S0967-0645\(01\)00041-8](https://doi.org/10.1016/S0967-0645(01)00041-8), 2001.
- Smith, C. R., Levin, L. A., Koslow, A., Tyler, P. A., and Glover, A. G.: The near future of the deep seafloor ecosystems, in: *Aquatic Ecosystems: Trends and Global Prospects*, edited by: Polunin, N. V. C., Cambridge University Press, 334–353, <https://doi.org/10.1017/CBO9780511751790.030>, 2008.
- Smith, K. L., White, G. A., and Laver, M. B.: Oxygen uptake and nutrient exchange of sediments measured in situ using a free vehicle grab respirometer, *Deep-Sea Res. Pt. II*, 26, 337–346, [https://doi.org/10.1016/0198-0149\(79\)90030-X](https://doi.org/10.1016/0198-0149(79)90030-X), 1979.
- Spickermann, R.: Rare Earth Content of Manganese Nodules in the Lockheed Martin Clarion-Clipperton Zone Exploration Areas, *Proc. Off. Technol. Conf.*, Houston Texas, 2012.
- Stratmann, T., Lins, L., Purser, A., Marcon, Y., Rodrigues, C. F., Ravara, A., Cunha, M. R., Simon-Lledó, E., Jones, D. O. B., Sweetman, A. K., Köser, K., and van Oevelen, D.: Abyssal plain faunal carbon flows remain depressed 26 years after a simulated deep-sea mining disturbance, *Biogeosciences*, 15, 4131–4145, <https://doi.org/10.5194/bg-15-4131-2018>, 2018.
- Thiel, H. and Forschungsverband Tiefsee-Umweltschutz: Evaluation of the environmental consequences of polymetallic nodule mining based on the results of the TUSCH Research Association, *Deep-Sea Res. Pt. II*, 48, 3433–3452, [https://doi.org/10.1016/S0967-0645\(01\)00051-0](https://doi.org/10.1016/S0967-0645(01)00051-0), 2001.
- Trueblood, D. D. and Ozturgut, E.: The benthic impact experiment: A study of the ecological impacts of deep seabed mining on abyssal benthic communities, *Proc. 7th ISOPE*, 481–487, 1997.
- Van Dover, C. L.: Tighten regulations on deep-sea mining, *Nature*, 470, 31–33, <https://doi.org/10.1038/470031a>, 2011.
- Vanreusel, A., Hilario, A., Ribeiro, P. A., Menot, L., and Arbizu, P. M.: Threatened by mining, polymetallic nodules are required to preserve abyssal epifauna, *Sci. Rep.-UK*, 6, 26808, <https://doi.org/10.1038/srep26808>, 2016.
- Volz, J. B., Mogollón, J. M., Geibert, W., Martínez Arbizu, P., Koschinsky, A., and Kasten, S.: Natural spatial variability of depositional conditions, biogeochemical processes and element fluxes in sediments of the eastern Clarion-Clipperton Zone, Pacific Ocean, *Deep-Sea Res. Pt. I*, 140, 159–172, 2018.
- Volz, J. B., Haffert, L., Haeckel, M., Koschinsky, A., and Kasten, S.: Solid-phase TOC and bulk Mn data for sediment cores taken in small-scale disturbance tracks during SONNE cruise SO239 in the Clarion-Clipperton Zone (CCZ), <https://doi.org/10.1594/PANGAEA.904560>, 2019a.
- Volz, J. B., Haffert, L., Haeckel, M., Koschinsky, A., and Kasten, S.: Porosity data for sediment cores taken in small-scale disturbance tracks and undisturbed reference sites during SONNE cruise SO239 in the Clarion-Clipperton Zone (CCZ), <https://doi.org/10.1594/PANGAEA.904578>, 2019b.
- Volz, J. B., Liu, B., Köster, M., Henkel, S., Koschinsky, A., and Kasten, S.: Post-depositional manganese mobilization during the last glacial period in sediments of the eastern Clarion-Clipperton Zone, Pacific Ocean, *Earth Planet. Sc. Lett.*, 532, 116012, <https://doi.org/10.1016/j.epsl.2019.116012>, 2020.
- Wedding, L. M., Reiter, S. M., Smith, C. R., Gjerde, K. M., Kittinger, J. N., Friedlander, A. M., Gaines, S. D., Clark, M. R., Thurnherr, A. M., Hardy, S. M., and Crowder, L. B.: Managing mining of the deep seabed, *Science*, 349, 144–145, 2015.
- Widmann, P.: Enrichment of mobilizable manganese in relation to manganese nodules abundance, Master thesis, Eberhard Karls Universität Tübingen and the Federal Institute for Geoscience and Resources, Hannover, 182 pp., 2015.
- Zonneveld, K. A. F., Versteegh, G. J. M., Kasten, S., Eglinton, T. I., Emeis, K.-C., Huguet, C., Koch, B. P., de Lange, G. J., de Leeuw, J. W., Middelburg, J. J., Mollenhauer, G., Prahl, F. G., Rethemeyer, J., and Wakeham, S. G.: Selective preservation of organic matter in marine environments; processes and impact on the sedimentary record, *Biogeosciences*, 7, 483–511, <https://doi.org/10.5194/bg-7-483-2010>, 2010.